

# Complexity Leads to Simplicity: A Consensus Layer V Pyramidal Neuron Can Sustain Interpulse-Interval Coding

Chandan Singh<sup>1</sup>, William B Levy<sup>1\*</sup>

<sup>1</sup> Departments of Neurosurgery and of Psychology, University of Virginia, Charlottesville, VA, USA.

\* Corresponding author

Email: [wbl@virginia.edu](mailto:wbl@virginia.edu)

## Abstract

In terms of a single neuron's long-distance communication, interpulse intervals (IPIs) are a possible alternative to rate and binary codes. As a proxy for IPI, a neuron's time-to-spike (TTS) can be found in the biophysical and experimental literature. Using the current, consensus layer V pyramidal neuron, the present study examines the feasibility of IPI-coding and examines the noise sources that limit the information rate of such an encoding. In descending order of noise intensity, the noise sources are (i) synaptic variability, (ii) sodium channel shot-noise, followed by (iii) thermal noise with synaptic noise much greater than the sodium channel-noise. More importantly, the biophysical model demonstrates a linear relationship between input intensity and  $TTS^{-1}$ . This linear observation contradicts the assumption that a neuron should be treated as a passive, electronic circuit (an RC circuit, as in the Stein model). Finally, the biophysical simulations allow the calculation of mutual information, which is about 3.0 bits/spike.

## Author Summary

In order to obtain a complete understanding of neural computation and communication, it is necessary to understand how one neuron communicates with another. To create a quantitative understanding of such communication, we need to understand the neural code. One possible code is referred to generically as a spike-timing code, or in a more technical way, an interpulse interval code. We use a biophysical model of a neocortical pyramidal neuron consisting of an appropriate morphology and known voltage-activated channels to qualify this neuron's time-to-spike in response to current injections or simulated synaptic inputs. This biologically appropriate and biophysically complex has a simple linear characterization necessary for interpulse interval coding, a characterization not demonstrated by the simpler passive model often used by neurotheoreticians. Thus, we have an example where biophysical complexity at the level of voltage-activated channels leads to input-output simplicity at the level of a neuron's encoding of information.

## Introduction

This study addresses three contemporary topics aimed at understanding neural computation and neural codes: (1) Is the leaky integrate-and-fire neuron a better model than a neuron using linear additivity to reach threshold? (2) What are the relative contributions of the stochastic processes that limit information flow across a neuron? And (3) what is the

bits-per-spike mutual information capability of a neocortical pyramidal cell using a recent biophysical model of this neuron's spike-generation?

McCulloch and Pitts introduce the computational neuron as a deterministic threshold-linear device [1]. Gerstein and Mandelbrot consider a linearly additive neuron in a stochastic setting [2]. However, even in this novel work which assumes an additive neuron, there is the absence of whole-hearted support for linearity because of a neuron's known leak-currents. Indeed, although there has been some biophysical modeling that attempts to justify a linear neuron [3-5], much effort has gone into understanding the stochastic, leaky-neuron model and its generation of an interpulse interval via first hitting-time [6-13].

For neurons functioning within cortical brain circuitry, there is support for a neuron that performs linear integration [14-16]. It has been suggested that nonlinear conductances can offset certain sublinear processes [3]. It has been recognized for more than a quarter of a century that the non-linearity offered by voltage-controlled channels can take a sublinear neuron and linearize it, at least in terms of loss of synaptic drive. More recently, preliminary biophysical models can compensate for time-dependent leak [17]. As shown below, this linear hypothesis exists over a limited range, for a biophysical model that accurately fits demanding neurophysiological data concerning the shape and initiation site of the action potential [18]. In particular, the recent biophysical model [19] of a non-stochastic neuron demonstrates a certain restricted linearization. In this context, the neuron selected here seems to be the "consensus pyramidal neuron" with several labs using the model consensus morphology [20-23] and further the same VGCs [19,24] with agreement in terms of the variety and placement of voltage-activated conductances. It includes, in addition to a voltage-controlled K-channel, two types of voltage-controlled Na-channels (Nav 1.2 and Nav 1.6) with a particular microscopic distribution, notably a high concentration of the low-threshold Nav 1.6 in the initial segment of the axon (AIS) [25-28].

Here the deterministic model (continuous Na-channel conductance as a function of voltage) is the starting point of the model. Then, after evaluating the inverse relationship between injected current and time-to-spike, a stochastic model subject to Na-channel shot activations is investigated. This neuron is activated in two different ways: with a noise-free current-step and with a random point-process. Considering three noise processes — thermal, Na-channel shots, and synaptic activation shots — synaptic noise seems to be the only quantitatively meaningful noise-source. It is fairly well-established that synaptic noise dominates [29] and that the most dominant source of noise

besides electrical noise is channel-noise [30-32]. Interest seems to center on sodium channel noise, as this is believed to be the largest [33].

Previous calculations of mutual information that indirectly evaluate the effect of intrinsic noise use the HI model [34]. This model assumes a Gaussian input and a Gaussian output. Such an assumption might be appropriate for a visual world in motion, but does not seem appropriate for the problem of transmitting information of scene analysis during visual fixations. For such problems one can propose the existence of a scalar latent variable and a conjectured output code. With these two hypotheses, Shannon's mutual information should consider the transmission of a scalar latent variable that parameterizes a Poisson process as the input while the encoded output of the neuron is interpulse interval. We consider the information throughput of a contemporary biophysical model of a neocortical pyramidal neuron and analyze it in a region that approximates the interpulse interval encoding of a neuron.

Such a noise analysis may or may not be intrinsically interesting, but we contend that the role such noise plays in the bit-rate of a neuron is a matter of interest. Typically, (for another method, see [34]) to analyze the bit-rate via Shannon's mutual information requires a statement of the code (an input and an output variable) and a quantitative understanding how stochastic aspects affect transmitting an input value via this code. At the extreme, it is well understood that thermal noise will always keep mutual information finite. However, more precise statements require much better knowledge of all the relevant stochastic processes and some amount of biophysics. Here, using the biophysical model, the mutual information is estimated to be about 3.0 bits per spike.

## Results

### Linearized inverse time-to-spike

The physiological origin of the Hu et al model seems based on a very narrow band of current-step intensities. In fact, the model sustains an inverse linear range for current-steps ranging from 0.51 nA to 0.85 nA when there is the requirement that action potential initiation begins at the AIS; relaxing this last requirement extends the range ever so slightly (the upper bound becomes 1.0 nA). Fig 1 illustrates this inverse relationship. Fig 1A uses the point-injection of a current-step. In this case the slope is  $0.30 \mu\text{C}^{-1}$  with an extrapolated y-intercept at zero-current of  $-0.13 \text{ ms}^{-1}$ . When spatially-distributed synaptic activation produces the action potential, the slope is  $0.0028 \text{ events}^{-1}$  with a zero-intensity intercept of  $-0.09 \text{ ms}^{-1}$ . Perhaps due to the none point-nature of synaptic activation, the currents required to fire using synaptic activation are consistently larger than the point current

injections. That is, assuming a current-step of 1 nA, dividing by a driving voltage of 50 mV, then dividing by the synaptic conductance of 200 pS, and finally dividing by the synaptic event duration of 1.2 ms, yields 83.3 events / ms.

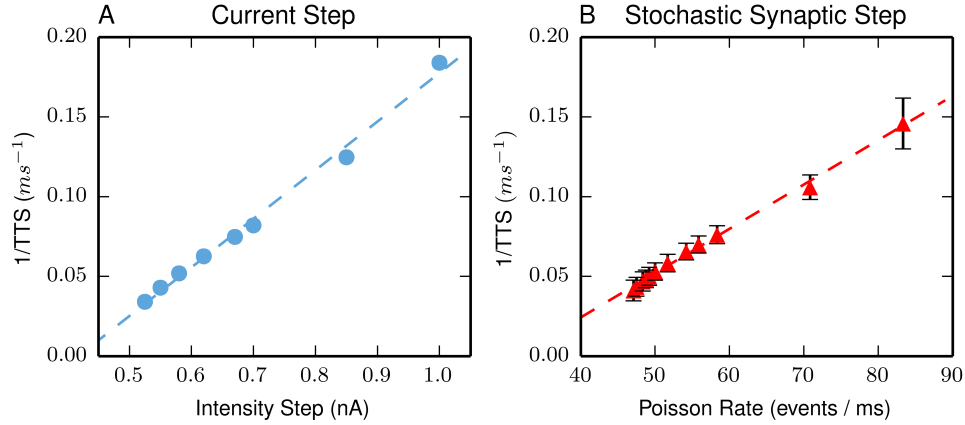


**Fig 1. A linear inverse TTS as a function of excitation.** Excitation is either (A) a point dendritic current-step or (B) a spatially dispersed, synaptic activation. Lines are best linear fits (see text). Each point is an average of 120 excitations from rest. The error bars (SEM) for the current-step are within the plot points. All points but the highest intensities always had spike initiation at the AIS. At the largest intensity on each curve, the spike originated in the dendrite 20 percent of the time.

### Variation in TTS

The overriding variation of the TTS using synaptic activation arises from the variability of the stochastic process itself. This conclusion is best seen by comparing the histogram of TTS for a deterministic current-step to the stochastic synaptic activation step.

For the highest intensities, the ratio of the variances is more than 200, while for the lowest intensities the ratio of the variances is more than 40. The standard deviations are plotted in Fig 2 for better visualization of the size of this effect as a function of inverse intensity (note when viewing these curves, the leftmost values of TTS correspond to the highest intensities). The noise increases as the TTS increases; this is mostly because the number of events needed to fire a spike increases with the TTS. In addition, threshold starts to rise. Such a greater amount for depolarization means that more sodium channels need to be activated at threshold. This larger number of sodium channels correlates with a larger standard deviation. Nevertheless, there is no spontaneous firing in this neuron; the contribution of an individual

channel fluctuation of sodium is not enough to fire the neuron until the neuron is very close to threshold.

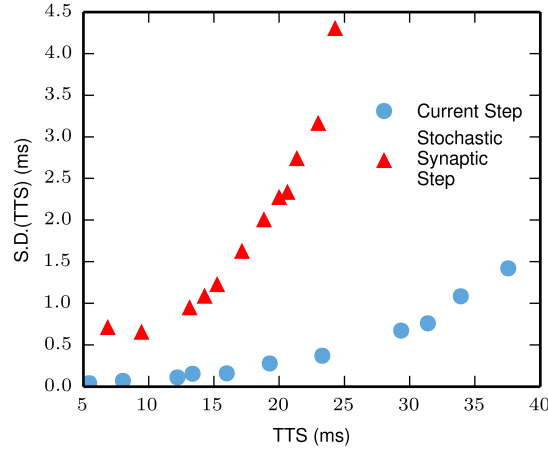


**Fig 2. Synaptic activation increases variation.** The only variation in TTS using a current-step is due to the stochastic nature of Na-channel activation. Random synaptic activation greatly increases the variation in TTS. Plot points correspond to the reverse-ordered successive intensities of Fig 1.

As is well-known for additive point processes, a larger number of events with smaller values (conductances) leads to lower average variance of the steady-state voltage. This lower variance in the voltage is reflected as lower variance in the TTS. A simple model of this relationship between steady-state variance of the voltage and the variance of the TTS (as a first hitting-time distribution) is seen in the standard result [35] that the variances of a first hitting-time and of a Brownian motion (which shot noises can approximate) are proportional.

As one would expect, maintaining a constant total conductance while changing the pS/event changes the variance. In fact, there is a linear relationship between the size of the individual conductance event and the variance (see Fig 3). The best linear fit for Fig 3A is  $\text{Var}[\text{TTS}] = 0.0012 \cdot x + 0.003$  with an  $R^2$  value of 0.984 and the fit for Fig 3B is  $\text{Var}[\text{TTS}] = 0.0052 \cdot x - 0.0797$  with an  $R^2$  value of 0.993. The conductance of a sodium channel is in the vicinity of 10 – 20 pS [36-38], while the conductance of a synapse is about 200 pS. Synaptic noise dominates, even when varying the parameters of the model (ex. pS/channel, pS/synapse). When combining both sources of noise, the noise is indistinguishable from the noise generated only by the synaptic input.

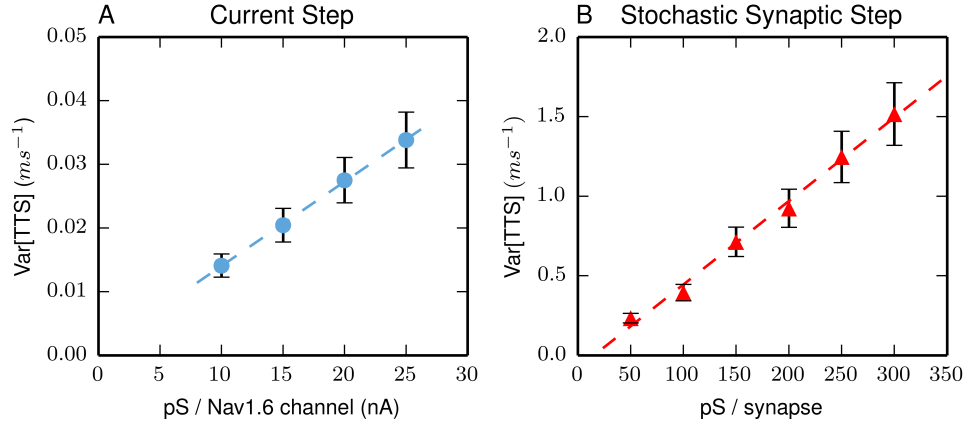


**Fig 3. Synaptic shot-noise far exceeds Na-channel shot-noise** (note the y-axis scale differences). (A) is a current-step of 0.7 nA and (B) has  $\lambda=58.3$  events/ms for a mean pS/synapse of 200. TTS variance increases as conductance events get larger while keeping  $\bar{g}$  constant. Fixed synaptic excitation at 200 pS/synapse results in  $\text{Var}[\text{TTS}]=0.92 \text{ ms}^2$ . Although variance in shot-noise sums should increase as the square root of increasing individual conductances, TTS variance is linear. Error bars are SEM. Lines are best linear fits (see text).

Finally, as will be important in the next section, it is necessary to have reliable probability distributions for the relationship between intensity and TTS. Fig 4 again shows that synaptic variation swamps sodium channel-induced variation (whatever noise is produced in the current-step histogram is incorporated into the stochastic synaptic step). However, more to the point is that the TTS distribution can be fit by an inverse Gaussian distribution (see Fig 4).

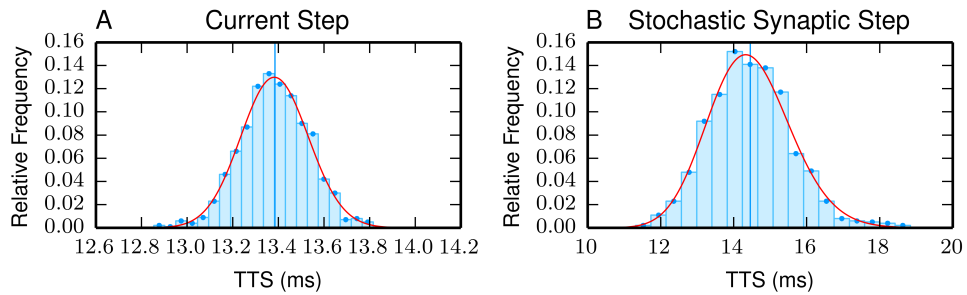


**Fig 4. TTS relative frequency histogram and overlaid inverse Gaussian distribution** with the same mean and variance. (A) Using a current-step of .67 nA, the mean TTS is 13.38 ms (vertical line) and the variance is  $0.022 \text{ ms}^2$ . (B) Using Poisson synaptic activation ( $\lambda=55.8$  events/ms), the mean TTS is 14.46 ms (vertical line) and the variance is  $1.25 \text{ ms}^2$ . 1,000

simulations produce each of the histograms. Current and synaptic activations begin at TTS=0. Notice the scale difference.

### Thermal Noise

Thermal noise is also present, but it is the noise source of least concern. Although thermal noise increases with increasing resistance, the low-pass property of a resistive-capacitive circuit when recording across the capacitor exactly cancels out the increase in thermal noise by lowering the high-frequency cutoff of the filter [39 p352]. Thus, the thermal noise (calculated as the expected value of the variance of the voltage) is equal to  $kT / C = 1.78 \times 10^{-11} \text{ V}^2$  ( $C$  is the capacitance of the neuron, 240 pF;  $k$  is the Boltzmann constant; and  $T$  is body temperature, 310 K). Thus, the standard deviation of this zero-centered noise is 4.22  $\mu\text{V}$ . Compare this value to the shot noise fluctuations shown in Fig 5 inset; it is much smaller than the sodium channel shot-noise.

### I( $\Lambda$ ;TTS)

Treating the neuron as an information channel, we identify the input random variable as  $\Lambda$  and the output random variable as TTS. A proper calculation requires an appropriate range for both of these random variables. As in the fit to the histogram (Fig 4), the assumed range of TTS is the positive real line; however, as one can see in Fig 4, the probability of long and short durations is miniscule. Even though the earlier results demonstrate an expanded range for the intensities of synaptic activation beyond those reported by Hu et al, this range seems overly modest for a pyramidal neuron of neocortex whose average activity is under 10 Hz, implying an average firing time between pulses of more than 100 ms. Regardless of the biophysical failings of the model, an appropriate approximation for a meaningful mutual information requires us to extend the range of synaptic intensities beyond those values appearing in Fig 1. Therefore, we extended the range on the low-intensity end to 200 ms. The effect this has on the mutual information calculation is shown in S3 Fig.

Since we do not know the probability distribution for  $\Lambda$ , we compare the result for three different distributions. The distributions and each of their associated mutual information values are summarized in Table 1. The calculation is described in detail in the methods section.

**Table 1 Distributions for  $\Lambda$  and associated mutual information values.**

Distributional Form	Distribution	$E[\Lambda]$ (events/ ms)	$H(T)$ (bits/spike)	Mutual Information (bits/spike)
$c/\lambda$	$1.07 / \lambda$	54.2	5.88	3.00
$c$	0.020	58.1	5.37	2.77
$\frac{Exp(-\lambda / c)}{c \cdot [Exp(-\lambda_{\min} / c) - Exp(-\lambda_{\max} / c)]}$	$\frac{Exp(-\lambda / 100)}{28.59}$	55.9	5.94	2.99

Common to all distributions is the range of  $\Lambda$ :  $\lambda \in [32.78, 83.33]$ .

## Discussion

### Linearity

The fitting of the inverse Gaussian distribution and linearization is important in the historical context of neuron modeling. It is a pervasive assumption in many computational models, dating back to McCulloch and Pitts [1], that linear computation (or log-linear) in fact, is assumed and seemingly required for several recent models [40-42]. As a first qualification of linear integration and interspike interval (ISI) coding, the inverse of the TTS should be linearly related to the intensity of the current-step. Previously, an earlier model of a simplified neuron model used voltage-gated conductances to demonstrate linear charging due to the added voltage-dependent nonlinearities [17]. The idea of a neuron with nonlinear, voltage-activated conductances is at odds with the textbook RC neuron whose synaptic excitation is interpreted as an Ornstein-Uhlenbeck process [7-12,43]. Until proved otherwise, it seems safe to assume that all excitatory neocortical neurons contain voltage-activated conductances.

The results show that over a limited range of intensities this model produces the desired inverse relationship between intensity and TTS (Fig 1) in a consensus pyramidal model, and these observations were made without manipulating the model's values and placements of voltage-gated conductances. Additionally, the model produces an inverse Gaussian distribution for the TTS (Fig 4). Indeed, this idea of the inverse Gaussian and the linearity required of the excitation process is actually quite old (a result first pointed out in neuroscience by Gerstein and Mandelbrot) [2]. This result is available to an Ornstein-Uhlenbeck diffusion, but only as an approximation of a diffusion that runs for a very short time [44]. In sum, the observations

here are a prime example of complexity (the voltage-activated conductances) leading to simplicity (linear additivity producing a closed-form probability hitting time distribution).

### Sources of Noise

Some recent reviews have speculated on various qualitative sources of noise [43-46]. Here we are concerned with a more precise, quantitative statement than these qualitative speculations. Historically, perhaps the earliest measurement in estimation of noise sources is found in [29], who suggest that synaptic noise can account for all the variability in ISIs. Because their observations were performed *in vivo*, their results cannot directly isolate the noise contributions from the synaptic input and channel noise; however, the observations here are able to do so (Fig 3). Even more recent results do not contradict the idea that synaptic noise dominates over channel-noise sources [49]. Although their results suggest non-Poisson inputs, these results and the interpretations are consistent with synaptic variability dominating VAC shot-noise variability in the physiological situation. In that study, the input excitation of the neuron creates a near steady-state situation (current applications last for at least a second). These long-duration stimuli will produce very different effects than our very short current applications that are of most relevance for studying TTS.

Under a very different set of assumptions, Sengupta et al. [50] also conclude that VAC shot-noise is only a minor and possibly ignorable source of input-output variability. Two distinctions stand out when comparing their results to the current study. Their model neuron is a biophysical neuron but relative to the one studied here seems somewhat arbitrary in its construction. The neuron used here is the consensus layer 5 pyramidal neuron (see third paragraph of introduction for references). Second, they model a dynamic input signal, perhaps inspired by the fly eye research that used a Gaussian input signal and symbolic decoding [34,51]. In contrast, the neuron of interest here can be thought of as performing computation (perhaps discrimination) over the interval of a visual fixation. In this case, we must suppose a prior distribution. Because we don't know the correct distribution, we offer three possibilities each of which is compatible with the dynamic range of the neuron being studied. Of course, any calculation of mutual information must make an assumption about the long-term prior distribution of the input intensity ( $\Lambda$ ) for the neuron under study.

While it is certainly true that noise limits the detection by peripheral sensors (hair cells in the basal ganglia, cones in the eye, etc.), we speculate that randomization processes rather than classic versions of noise itself are of

much more concern in calculating information transmitted between neurons than explicit noise processes including thermal noise and shot noise of voltage-activated conductances. Other types of noise might include chaotic oscillations generated by interactions between voltage-activated conductances, but we assume in pyramidal cell neocortical computation there are no such oscillations. Thus, rather than calling the unpredictable firing of a neuron noise, we might use the term randomization, which is produced by the large number of poorly synchronized, input-line activations. Moreover, any such randomization process which itself is enhanced by quantal synaptic failure [52].

### **Mutual Information**

Our estimate of mutual information agrees with the approximately 3 bits per spike calculated by [34]. Indeed, this agreement might be somewhat surprising considering how large a dynamic range they used versus how restricted the dynamic range is for the pyramidal neuron studied here. Other estimates range from 2 – 5 bits per spike [53-60]; see [61] for a review.

It can be argued that the 3-bit calculation here is an underestimate due to the constraints imposed on the consensus neuron being used. For example, the model considered here sustains firing only over a limited range of input intensities, and a more accurate neuron with more voltage-activated conductances (e.g. the  $I_h$  conductance or even a large set of spatially-distributed conductances [62]) might lead to a neuron that has a greater dynamic range. Another limitation of the current study is a lack of inhibition. Physiologically, a neocortical neuron will simultaneously receive inhibition and excitation. Such inhibition downgrades the effect of synaptic events, which in turn requires larger values of  $\Lambda$  to produce the same firing rates ( $\Lambda$ ). By increasing the number of events per output spike, the information rate per output spike goes up. For example, a four-fold increase in the number of events needed to fire the neuron increases the mutual information by about 1 bit / spike.

Other assumptions affect the calculation of mutual information. Stochastic  $K^+$  channels could contribute to the variance of the TTS, thus decreasing mutual information. However, the TTS reflects variability occurring at low amounts of depolarization compared to when voltage-dependent  $K^+$  channels tend to be activated. Additionally,  $K^+$  channels can have smaller single-channel conductances than the  $Na^+$  channels used here [63-65], and thus their noise contribution will be smaller.

## Suggestions for future research

This research invites more research into the linear model of the neuron. As a relatively simple alternative to the stochastic, leaky-neuron model, the linear model can provide insights into neural computation, even in up-to-date, realistic physiological models. Before going further with this model neuron, experimental scientists should evaluate the spike-generating characteristics of this layer V neuron over a wider range of conditions. These conditions include both higher and lower levels of excitation, excitation in the presence of inhibition, and TTS relationships after a preceding spike.

## Methods

### Model

The cell that is modeled is a Layer 5 pyramidal cell quantified by Mainen & Sejnowski [20] (their Fig 1D). The biophysical model evolved from [65] in which it was used to study back propagating action potential spikes. This led to [19] in which it was further refined (model can be retrieved from ModelDB [66]). The model was fit to measurements at several different places on the neuron including the AIS, axon, and dendrites.

The model includes both Nav 1.6 and Nav 1.2 channels distributed along the AIS. It is well-accepted that the action potential is initiated at the distal AIS [26-27,67] with its high concentration of different sodium channel types [25,28,68]. The capacitance in the soma was changed from  $1 \mu\text{F}/\text{cm}^2$  to  $.9 \mu\text{F}/\text{cm}^2$ , as this is a more realistic value [69]. In addition, a small amount of persistent Na channels was added at the proximal apical dendrite to simulate more realistic neuronal firing over a longer range of times. The persistent sodium channels were modelled using the Nav1.6 channels with shifted inactivation rate equations, so that they would inactivate much more slowly [38,67,70].

The main change was to alter the sodium channels so that they operated stochastically. The stochastic sodium channels were modeled with a widely-used eight-state kinetic reaction scheme describing the  $m^3h$  Hodgkin-Huxley activation kinetics [71-72] quantified in [73]. This gating scheme is shown in [74] (their Fig 4A). When run deterministically, there is no variability. These changes did not substantially change the overall shape of the action potential (Fig 5). The main difference is that the stochastic voltage-trace lies below the deterministic immediately before firing. Since it is noisier, the stochastic neuron can suddenly cross threshold with a stochastic event, and thus does not have to gradually increase to threshold as the deterministic neuron does. Thus, the stochastic neuron tends to be at a slightly lower voltage when it fires than the deterministic neuron.

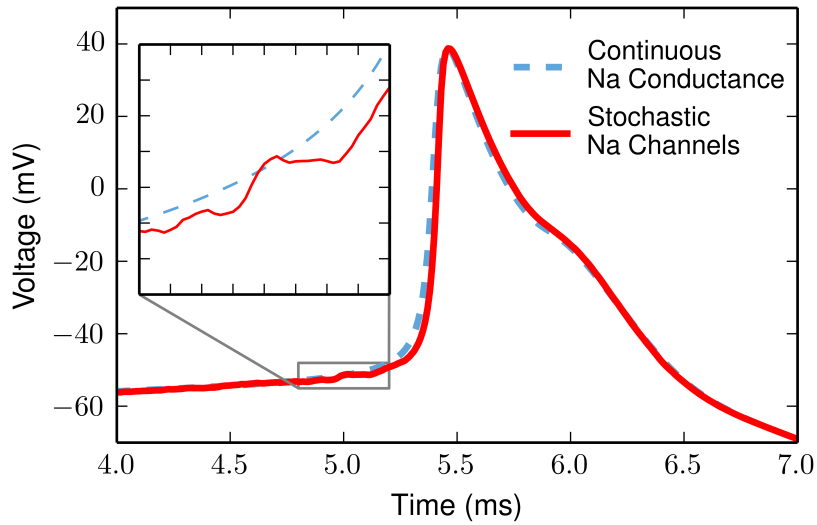


**Fig 5. Comparison of a stochastic- and a deterministic-based action potential.** The deterministic action potential (blue dashed line) reproduces the result of Hu et al; their action potential initiates at the AIS and spreads to the soma and apical dendrite. Aligned, peaked to peak, is a second action potential (solid red line) using stochastic Na-channels (both Nav 1.2 and Nav 1.6). Both action potentials are generated by the same somatic current-step of 1 nA. Inset y-axis goes from -55 mV to -48 mV (increments of 1 mV); inset x-axis goes from 4.8 ms to 5.2 ms (increments of .05 ms).

### Excitation

Simulations were performed using the simulation environment *NEURON* [75]. A time step of 1  $\mu$ s was used, and the results did not change for smaller time steps. In all cases, the neuron is allowed to come to steady state before the stimulus is applied. The neuron was stimulated in the main apical dendrite 250  $\mu$ m from the soma because this is where synapses are located, and our aim was to study the noise in the synaptic input. This was done in two ways: first with a noise-free current-step in the main apical dendrite, and second by simulating synaptic activity. Synaptic activity was simulated using synapses distributed evenly along the main apical dendrite 200  $\mu$ m-300  $\mu$ m from the soma. Synapses were simulated as the Poisson arrival of square pulses of 200 pS that lasted 1.2 ms with a reversal potential of 0 mV. The Poisson assumption used here arises not from a Poisson assumption on individual inputs, but the Poisson approximation [76] produced by the unioning of all the input lines, each one being a point process.

As a surrogate for interpulse interval, the time-to-spike (TTS) is measured for current-step and for step random synaptic activations. The TTS

is defined as the time it takes to achieve maximum voltage from steady state. This is used because we require a clean system for quantifying the noise effects of the sodium channel and the synaptic input fluctuations.

### Mutual Information Calculation

Treating the neuron as an information channel, we identify the input random variable as  $\Lambda$  and the output random variable as TTS. In order to calculate the mutual information  $I(\Lambda; \text{TTS})$  we require three probability distributions:  $P(\Lambda)$ ,  $P(\text{TTS}|\Lambda)$ , and  $P(\text{TTS})$ .

**P( $\Lambda$ ).** We choose the distribution of  $P(\Lambda)$  over the range we are studying. Since we do not know the probability distribution for  $\Lambda$ , we try multiple different distributions.

**P( $\text{TTS}|\Lambda$ ).** We have seen that at a given intensity  $\lambda$ , the distribution of TTS follows an inverse Gaussian distribution (Fig 2). The PDF of the inverse Gaussian distribution with a mean of  $\mu$  and a shape parameter of  $\rho$ .

$$IG(\mu, \rho) = \left( \frac{\rho}{2\pi TTS^3} \right)^{1/2} \exp \left( \frac{-\rho(TTS - \mu)^2}{2\mu^2 TTS} \right) \quad (1)$$

The shape parameter  $\rho = \mu^3 / \sigma^2$ , where  $\sigma^2$  is the variance of TTS. To get an expression for  $P(\text{TTS}|\Lambda)$ , we require the parameters  $\mu$  and  $\rho$  for any  $\lambda$  in our range. To find  $\mu$  as a function of  $\lambda$  ( $\mu(\lambda)$ ), we do an inverse best-fit to the collected data on  $\lambda$  vs.  $E[\text{TTS}]$ , and to find  $\sigma^2$  as a function ( $\sigma^2(\lambda)$ ), we do an inverse best-fit to the collected data on  $\lambda$  vs.  $\text{Var}[\text{TTS}]$ . If we need to extrapolate the variance past the range of collected data, we use the largest observed variance (18.57 ms<sup>2</sup>). All fitting data is in S1 Table. Then we can define  $P(\text{TTS}|\Lambda)$ .

$$P(\text{TTS} | \Lambda) = IG \left( \mu(\lambda), \frac{\mu(\lambda)^3}{\sigma(\lambda)^2} \right) \quad (2)$$

**P( $\text{TTS}$ ).**  $P(\text{TTS})$  is computed by numerical integration over the entire range of  $\Lambda$  under consideration. The resulting  $P(\text{TTS})$  distributions are shown in S4 Fig.

$$P(\text{TTS}) = \int_{\lambda_{\min}}^{\lambda_{\max}} P(\text{TTS} | \Lambda = \lambda) \cdot P_{\Lambda}(\lambda) d\lambda \quad (3)$$

**I( $\Lambda; \text{TTS}$ ).** The mutual information (in bits / spike) is calculated according to the following equation by summing over  $\Lambda$  with steps of .1 events/ms and by summing over TTS in the range [1 ms, 250 ms] with steps of 0.05 ms.

$$I(\Lambda; \text{TTS}) = \int_{32.78}^{83.33} P_{\Lambda}(\lambda) \int_0^{\infty} P(\text{TTS} | \Lambda) \log_2 \frac{P(\text{TTS} | \Lambda = \lambda)}{P(\text{TTS})} d\text{TTS} d\lambda \quad (4)$$

## Acknowledgements

We thank Costa Colbert for helpful suggestions and comments during the research and the writing of the manuscript. We also thank the Department of Neurosurgery for their support. This work was supported by the National Science Foundation 1162449 – Toby Berger & William Levy.

## References

1. McCulloch WS, Pitts W. A logical calculus of the ideas immanent in nervous activity. *The bulletin of mathematical biophysics*. 1943 Dec 1;5(4):115-33.
2. Gerstein GL, Mandelbrot B. Random walk models for the spike activity of a single neuron. *Biophysical journal*. 1964 Jan;4(1 Pt 1):41.
3. Bernander OJ, Koch C, Douglas RJ. Amplification and linearization of distal synaptic input to cortical pyramidal cells. *Journal of neurophysiology*. 1994 Dec 1;72(6):2743-53.
4. Morel D, Levy WB. Persistent sodium is a better linearizing mechanism than the hyperpolarization-activated current. *Neurocomputing*. 2007 Jun 30;70(10):1635-9.
5. Morel D, Levy WB. Cost of linearization for different time constants. *BMC Neuroscience*. 2008 Jul 11;9(Suppl 1):P52.
6. Ricciardi LM, Sacerdote L. The Ornstein-Uhlenbeck process as a model for neuronal activity. *Biological cybernetics*. 1979 Mar 1;35(1):1-9.
7. Giorno V, Lánský P, Nobile AG, Ricciardi LM. Diffusion approximation and first-passage-time problem for a model neuron. *Biological cybernetics*. 1988 May 1;58(6):387-404.
8. Capocelli RM, Ricciardi LM. Diffusion approximation and first passage time problem for a model neuron. *Kybernetik*. 1971 Jun 1;8(6):214-23.
9. Lánský P, Rospars JP. Ornstein-Uhlenbeck model neuron revisited. *Biological cybernetics*. 1995 Apr 1;72(5):397-406.
10. Lánský P, Sacerdote L. The Ornstein–Uhlenbeck neuronal model with signal-dependent noise. *Physics Letters A*. 2001 Jul 2;285(3):132-40.
11. Lánský P, Smith CE, Ricciardi LM. One-dimensional stochastic diffusion models of neuronal activity and related first passage time problems. *Trends in Biological Cybernetics*. 1990;1:153-62.
12. Stein RB. A theoretical analysis of neuronal variability. *Biophysical Journal*. 1965 Mar;5(2):173.
13. Tuckwell HC, Ditlevsen S. The space-clamped Hodgkin-Huxley system with random synaptic input: inhibition of spiking by weak noise and analysis with moment equations. *arXiv preprint arXiv:1604.04796*. 2016 Apr 16.

14. Carandini M, Heeger DJ, Movshon JA. Linearity and normalization in simple cells of the macaque primary visual cortex. *The Journal of Neuroscience*. 1997 Nov 1;17(21):8621-44.
15. Cash S, Yuste R. Input summation by cultured pyramidal neurons is linear and position-independent. *The Journal of neuroscience*. 1998 Jan 1;18(1):10-5.
16. Cash S, Yuste R. Linear summation of excitatory inputs by CA1 pyramidal neurons. *Neuron*. 1999 Feb 28;22(2):383-94.
17. Morel D, Levy WB. Interspike intervals under the constraint of linear synaptic integration and background synaptic activity. *BMC Neuroscience*. 2013 Jul 8;14(Suppl 1):P239.
18. Kole MH, Stuart GJ. Signal processing in the axon initial segment. *Neuron*. 2012 Jan 26;73(2):235-47.
19. Hu W, Tian C, Li T, Yang M, Hou H, Shu Y. Distinct contributions of Nav1. 6 and Nav1. 2 in action potential initiation and backpropagation. *Nature neuroscience*. 2009 Aug 1;12(8):996-1002.
20. Mainen ZF, Sejnowski TJ. Influence of dendritic structure on firing pattern in model neocortical neurons. *Nature*. 1996 Jul 25;382(6589):363-6.
21. Acker CD, Antic SD. Quantitative assessment of the distributions of membrane conductances involved in action potential backpropagation along basal dendrites. *Journal of neurophysiology*. 2009 Mar 1;101(3):1524-41.
22. Hallermann S, de Kock CP, Stuart GJ, Kole MH. State and location dependence of action potential metabolic cost in cortical pyramidal neurons. *Nature neuroscience*. 2012 Jul 1;15(7):1007-14.
23. Banitt Y, Martin KA, Segev I. A biologically realistic model of contrast invariant orientation tuning by thalamocortical synaptic depression. *The Journal of Neuroscience*. 2007 Sep 19;27(38):10230-9.
24. Platkiewicz J, Brette R. A threshold equation for action potential initiation. *PLoS Comput Biol*. 2010 Jul 8;6(7):e1000850.
25. Kole MH, Ilshner SU, Kampa BM, Williams SR, Ruben PC, Stuart GJ. Action potential generation requires a high sodium channel density in the axon initial segment. *Nature neuroscience*. 2008 Feb 1;11(2):178-86.
26. Baranauskas G, David Y, Fleidervish IA. Spatial mismatch between the Na<sup>+</sup> flux and spike initiation in axon initial segment. *Proceedings of the National Academy of Sciences*. 2013 Mar 5;110(10):4051-6.
27. Johnston D, Magee JC, Colbert CM, Christie BR. Active properties of neuronal dendrites. *Annual review of neuroscience*. 1996 Mar;19(1):165-86.

28. Colbert CM, Pan E. Ion channel properties underlying axonal action potential initiation in pyramidal neurons. *Nature neuroscience*. 2002 Jun 1;5(6):533-8.
29. Calvin WH, Stevens CF. Synaptic noise and other sources of randomness in motoneuron interspike intervals. *J Neurophysiol*. 1968 Jul 1;31(4):574-87.
30. Steinmetz PN, Manwani A, Koch C, London M, Segev I. Subthreshold voltage noise due to channel fluctuations in active neuronal membranes. *Journal of computational neuroscience*. 2000 Sep 1;9(2):133-48.
31. Van Rossum MC, O'Brien BJ, Smith RG. Effects of noise on the spike timing precision of retinal ganglion cells. *Journal of neurophysiology*. 2003 May 1;89(5):2406-19.
32. White JA, Rubinstein JT, Kay AR. Channel noise in neurons. *Trends in neurosciences*. 2000 Mar 1;23(3):131-7.
33. Schneidman E, Freedman B, Segev I. Ion channel stochasticity may be critical in determining the reliability and precision of spike timing. *Neural computation*. 1998 Oct 1;10(7):1679-703.
34. Bialek W, Rieke F, Van Steveninck RD, Warland D. Reading a neural code. *Science*. 1991 Jun 28;252(5014):1854-7.
35. Schrödinger E. *Statistical thermodynamics*. Courier Corporation; 1989.
36. Andrásfalvy BK, Magee JC. Changes in AMPA receptor currents following LTP induction on rat CA1 pyramidal neurones. *The Journal of physiology*. 2004 Sep 1;559(2):543-54.
37. Conti F, Hille B, Neumcke B, Nonner W, Stämpfli R. Measurement of the conductance of the sodium channel from current fluctuations at the node of Ranvier. *The Journal of physiology*. 1976 Nov 1;262(3):699-727.
38. Chatelier A, Zhao J, Bois P, Chahine M. Biophysical characterisation of the persistent sodium current of the Nav1.6 neuronal sodium channel: a single-channel analysis. *Pflügers Archiv-European Journal of Physiology*. 2010 Jun 1;460(1):77-86.
39. Papoulis A, Pillai SU. *Probability, Random Variables, and Stochastic Processes*. Probability, Random Variables, and Stochastic Processes, Fourth Edition, by Athanasios Papoulis and S. Unnikrishna Pillai. ISBN 978-0-07-366011-0. Published by McGraw-Hill Higher Education (a division of McGraw-Hill Companies), New York, NY USA, 2002.. 2002;1.
40. Deneve S, Pouget A. Bayesian multisensory integration and cross-modal spatial links. *Journal of Physiology-Paris*. 2004 Jun 30;98(1):249-58.
41. Barber MJ, Clark JW, Anderson CH. Neural representation of probabilistic information. *Neural Computation*. 2003 Aug;15(8):1843-64.

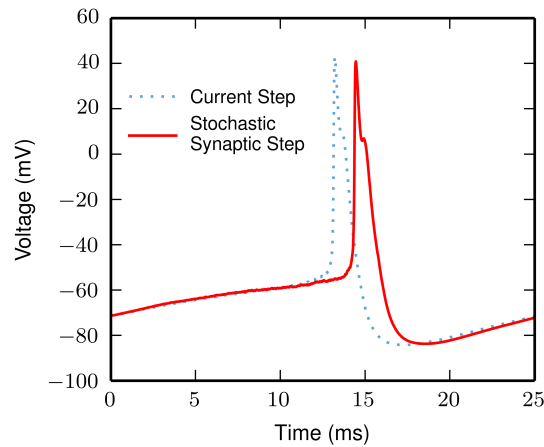
42. Levy WB, Colbert CM, Desmond NL. Elemental adaptive processes of neurons and synapses: a statistical/computational perspective. Erlbaum, Hillsdale, NJ; 1990.
43. Tuckwell HC. Introduction to theoretical neurobiology: volume 2, nonlinear and stochastic theories. Cambridge University Press; 2005 Sep 8.
44. Simen P, Balci F, Cohen JD, Holmes P. A model of interval timing by neural integration. *The Journal of Neuroscience*. 2011 Jun 22;31(25):9238-53.
45. Yarom Y, Hounsgaard J. Voltage fluctuations in neurons: signal or noise?. *Physiological reviews*. 2011 Jul 1;91(3):917-29.
46. Stein RB, Gossen ER, Jones KE. Neuronal variability: noise or part of the signal?. *Nature Reviews Neuroscience*. 2005 May 1;6(5):389-97.
47. Oprisan SA, Buhusi CV. What is all the noise about in interval timing?. *Philosophical Transactions of the Royal Society B: Biological Sciences*. 2014 Mar 5;369(1637):20120459.
48. Faisal AA, Selen LP, Wolpert DM. Noise in the nervous system. *Nature reviews neuroscience*. 2008 Apr 1;9(4):292-303.
49. Stevens CF, Zador AM. Input synchrony and the irregular firing of cortical neurons. *Nature neuroscience*. 1998 Jul 1;1(3):210-7.
50. Sengupta B, Laughlin SB, Niven JE. Consequences of converting graded to action potentials upon neural information coding and energy efficiency. *PLOS Comput Biol*. 2014 Jan 23;10(1):e1003439.
51. Nemenman I, Lewen GD, Bialek W, van Steveninck RR. Neural coding of natural stimuli: information at sub-millisecond resolution. *PLoS Comput Biol*. 2008 Mar 7;4(3):e1000025.
52. Levy WB, Baxter RA. Energy-efficient neuronal computation via quantal synaptic failures. *The Journal of Neuroscience*. 2002 Jun 1;22(11):4746-55.
53. Buracas GT, Zador AM, DeWeese MR, Albright TD. Efficient discrimination of temporal patterns by motion-sensitive neurons in primate visual cortex. *Neuron*. 1998 May 31;20(5):959-69.
54. Berry MJ, Meister M. Refractoriness and neural precision. *The Journal of Neuroscience*. 1998 Mar 15;18(6):2200-11.
55. Rieke F, Warland D, Bialek W. Coding efficiency and information rates in sensory neurons. *EPL (Europhysics Letters)*. 1993 Apr 10;22(2):151.
56. Rieke F, Bodnar DA, Bialek W. Naturalistic stimuli increase the rate and efficiency of information transmission by primary auditory afferents. *Proceedings of the Royal Society of London B: Biological Sciences*. 1995 Dec 22;262(1365):259-65.

57. Reinagel P, Reid RC. Visual stimulus statistics and the reliability of spike timing in the LGN. In Soc Neurosci Abstr 1998 (Vol. 24, p. 139).
58. Strong SP, Koberle R, van Steveninck RR, Bialek W. Entropy and information in neural spike trains. Physical review letters. 1998 Jan 5;80(1):197.
59. Warland DK, Reinagel P, Meister M. Decoding visual information from a population of retinal ganglion cells. Journal of Neurophysiology. 1997 Nov 1;78(5):2336-50.
60. Warland DK. Reading Between the Spikes: Real-Time Signal Processing in Neural Systems.
61. F. Rieke, D. Warland, R.R. de Ruyter van Steveninck. Spikes: Exploring the neural code. MIT Press, Cambridge, Mass., U.S.A., 1997.
62. Bahl A, Stemmler MB, Herz AV, Roth A. Automated optimization of a reduced layer 5 pyramidal cell model based on experimental data. Journal of neuroscience methods. 2012 Sep 15;210(1):22-34.
63. De Bruin, G., Guy, I., & Van den Berg, R. J. (1984). Single potassium channel conductance in the frog node of Ranvier. *Biophysical journal*, 45(4), 855.
64. Sakmann B, Trube G. Conductance properties of single inwardly rectifying potassium channels in ventricular cells from guinea-pig heart. The Journal of Physiology. 1984 Feb;347:641.
65. Yu Y, Shu Y, McCormick DA. Cortical action potential backpropagation explains spike threshold variability and rapid-onset kinetics. The Journal of Neuroscience. 2008 Jul 16;28(29):7260-72.
66. Hines ML, Morse T, Migliore M, Carnevale NT, Shepherd GM. ModelDB: a database to support computational neuroscience. Journal of computational neuroscience. 2004 Jul 1;17(1):7-11.
67. Palmer LM, Stuart GJ. Site of action potential initiation in layer 5 pyramidal neurons. The Journal of neuroscience. 2006 Aug 1;26(6):1854-63.
68. Royeck M, Horstmann MT, Remy S, Reitze M, Yaari Y, Beck H. Role of axonal NaV1.6 sodium channels in action potential initiation of CA1 pyramidal neurons. Journal of neurophysiology. 2008 Oct 1;100(4):2361-80.
69. Gentet LJ, Stuart GJ, Clements JD. Direct measurement of specific membrane capacitance in neurons. Biophysical Journal. 2000 Jul 31;79(1):314-20.
70. Rotaru DC, Lewis DA, Gonzalez-Burgos G. Dopamine D1 receptor activation regulates sodium channel-dependent EPSP amplification in rat

- prefrontal cortex pyramidal neurons. *The Journal of physiology*. 2007 Jun 15;581(3):981-1000.
71. Hille B. Ionic channels in excitable membranes. Current problems and biophysical approaches. *Biophysical Journal*. 1978 May;22(2):283.
  72. Hille B. Ion channels of excitable membranes. Sunderland, MA: Sinauer; 2001 Jul.
  73. Kole MH, Hallermann S, Stuart GJ. Single Ih channels in pyramidal neuron dendrites: properties, distribution, and impact on action potential output. *The Journal of neuroscience*. 2006 Aug 1;26(6):1677-87.
  74. Schmidt-Hieber C, Bischofberger J. Fast sodium channel gating supports localized and efficient axonal action potential initiation. *The Journal of Neuroscience*. 2010 Jul 28;30(30):10233-42.
  75. Carnevale NT, Hines ML. *The NEURON book*. Cambridge University Press; 2006 Jan 12.
  76. Barbour AD, Holst L, Janson S. *Poisson approximation*. Oxford: Clarendon Press; 1992 Feb.

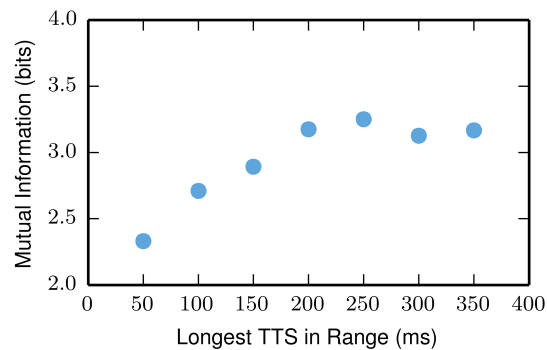
## Supporting Information

### S1 Table. Values for step intensity and recorded statistics on TTS



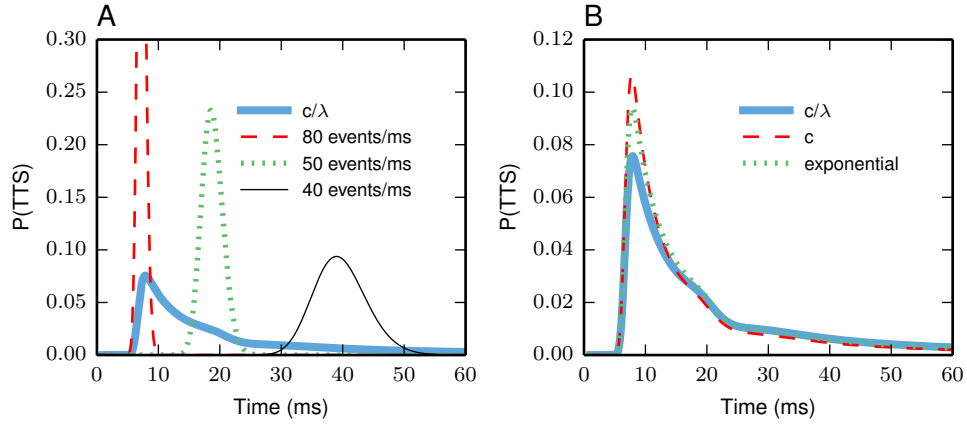
### S2 Fig. Voltage traces for a current-step and stochastic synaptic-step.

Voltage is measured at the AIS. Current-step is .7 nA and stochastic synaptic step is 58.33 events / ms. Though the average input current is the same, this stochastic step generally fires after this current step (see histograms in Fig 5) This delay occurs because the synaptic activations are distributed over a 100  $\mu\text{m}$  section of the dendrite while the current-step is a point source in the dendrite.



### S3 Fig. Mutual information values over different extrapolated ranges.

All calculations share the same shortest TTS (6.8 ms) and use the same distributional form for  $\Lambda$  ( $c/\lambda$ , where  $c$  is a constant). The maximum value of  $\lambda$  is 83.33 events / ms. The minimum value of  $\lambda$  changes depending upon the longest TTS in the range, and the value of  $c$  is chosen to normalize the distribution.



**S4 Fig.  $P(T)$  distributions.** (A) The  $P(\text{TTS})$  distribution (thick blue curve) is computed as the weighted sum of conditional distributions. Three conditional distributions  $P(\text{TTS}|\lambda)$  are shown for  $\lambda=80$  events/ms (red dashed line),  $\lambda=50$  events/ms (green dotted line), and  $\lambda=40$  events/ms (thin black line). (B)  $P(\text{TTS})$  resulting from different  $\Lambda$  distributions. Each distribution for  $T$  corresponds to a distribution for  $\lambda$  in Table 1.